

# Elastic Scattering of 160-MeV Protons from Be<sup>9</sup>, Ca<sup>40</sup>, Ni<sup>58</sup>, Sn<sup>120</sup>, and Pb<sup>208</sup>†

PHILIP G. ROOS\* AND N. S. WALL

Laboratory for Nuclear Science, Massachusetts Institute of Technology, Cambridge, Massachusetts  
and

Department of Physics and Astronomy, University of Maryland, College Park, Maryland

(Received 28 July 1965)

Using a good-resolution total-energy scintillation spectrometer, the elastic-scattering differential cross sections of 160-MeV protons from Be<sup>9</sup>, Ca<sup>40</sup>, Ni<sup>58</sup>, Sn<sup>120</sup>, and Pb<sup>208</sup> have been measured. Optical-model analyses of the data have been made, and the pertinent parameters are given. The most significant result of the analyses is that the extent of the imaginary part of the optical potential has a radius of the order of 10<sup>-13</sup> cm greater than that of the real part, independent of atomic weight.

## I. INTRODUCTION

ELASTIC-scattering experiments at relatively high energies are of interest in nuclear-structure studies for two reasons. Fundamentally, it is thought that the impulse approximation, along with a knowledge of nucleon-nucleon scattering (specifically, the two-body  $t$  matrix), can lead directly to an optical potential.<sup>1</sup> That is to say, within the framework of the impulse approximation, it is possible to represent the nucleon-nucleus interaction in terms of a single-body potential, derived from an appropriate average over the nucleon-nucleon scattering amplitudes. In a purely phenomenological sense it is useful to have an optical-model potential which accurately calculates elastic scattering. This potential can then be used in distorted-wave impulse or Born approximation calculations of direct reactions. Optical-model distortions have been used in inelastic scattering, pickup, and stripping reactions. The systematic behavior, observed in the present and other high-energy measurements, of the angular distributions, polarizations, and reaction cross sections, indicates the appropriateness of an optical-model description. On the other hand, it may not be possible to derive the detailed optical-model parameters from an impulse approximation or similar calculation at our present level of understanding. However, general orders of magnitude and trends with atomic weight should be comprehensible.

We have measured the differential cross sections for the elastic scattering of 160-MeV protons from a series of nuclei, and analyzed these data in terms of an optical-model calculation. Earlier, extensive elastic-proton-scattering work at 180 MeV had been performed by Johansson *et al.*,<sup>2</sup> and their data have recently been analyzed in detail by Satchler and Haybron.<sup>3</sup> There are also some early measurements at 95 and 160 MeV

by Gerstein<sup>4</sup> which have been analyzed in the WKB approximation. Earlier work has been summarized in the paper by Bjorkland *et al.* and in the book by Hodgson.<sup>5</sup>

## II. EXPERIMENTAL

For this experiment the 160-MeV unpolarized external proton beam of the Harvard University Cyclotron was used. The proton beam was stochastically extracted, giving a beam intensity of 10<sup>8</sup> → 10<sup>9</sup> protons/sec with a duty cycle of approximately 20%. The incident beam was monitored by a nonsaturating He ionization chamber.

The most difficult problem in high-energy nuclear-structure scattering experiments is in obtaining adequate energy resolution. Considerations of NaI(Tl) scintillation-counter pulse-height fluctuation phenomena led us to realize that it might be possible to achieve an energy resolution ( $\Delta E/E$ ) at these energies comparable to that of a magnetic spectrometer. We realized that the main problem would be the uniformity of light collection. To this end, we obtained a Harshaw<sup>6</sup> 3-in.×3-in. NaI crystal. This crystal was selected for uniform light collection, over the volume of the crystal, by scanning it with a low-energy  $\gamma$ -ray source. This selection produced a detector which gave a resolution of 1.35 MeV full width at half-maximum for 160-MeV protons. This resolution represented a significant improvement over similar detectors which had not been selected for uniform light collection.<sup>7</sup>

In addition to the NaI spectrometer, a counter telescope consisting of two thin plastic scintillators was used. A coincidence between the two plastic scintillators gated a multichannel analyzer which then stored the spectrometer pulse. This telescope defined the solid angle and greatly reduced the background. The angular resolution of the counter system was approximately  $\pm 0.5^\circ$ .

† This work at MIT was supported in part through funds provided by the Atomic Energy Commission under Contract No. AT(30-1)-2098. The work at the University of Maryland was supported in part by grants from the University Research Board.

\* This work was in part the doctoral thesis of P.G.R.

<sup>1</sup> A. K. Kerman, H. McManus, and R. M. Thaler, *Ann. Phys. (N. Y.)* **8**, 551 (1959).

<sup>2</sup> A. Johansson, U. Svanberg, and P. E. Hodgson, *Arkiv Fysik* **19**, 541 (1961).

<sup>3</sup> G. R. Satchler and R. M. Haybron, *Phys. Letters* **11**, 313 (1964).

<sup>4</sup> P. Gerstein, thesis, Harvard University, 1961 (unpublished).

<sup>5</sup> D. Bjorklund, I. Blandford, and S. Fernbach, *Phys. Rev.* **108**, 795 (1957); P. E. Hodgson, *The Optical Model of Elastic Scattering* (Oxford University Press, London, 1963).

<sup>6</sup> Harshaw Integral line counter from the Harshaw Chemical Corporation, Cleveland, Ohio.

<sup>7</sup> P. Roos, thesis, MIT, 1964 (unpublished); N. S. Wall and P. Roos, *Bull. Am. Phys. Soc.* **9**, 489 (1964).

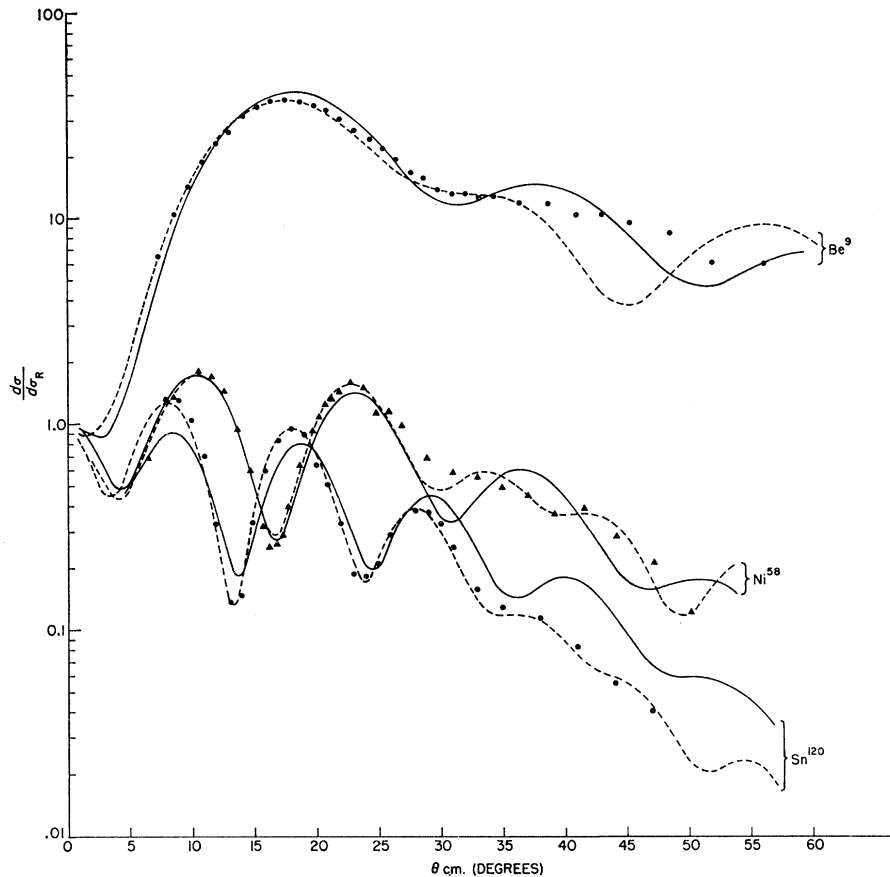


FIG. 1. The differential cross section for the scattering of 160-MeV protons from  $\text{Be}^9$ ,  $\text{Ni}^{58}$ , and  $\text{Sn}^{120}$  divided by point-charge scattering. The dashed lines are Satchler's optical-model analysis and the solid lines are the optical-model analysis by the authors. To avoid confusion the experimental errors have not been shown, but are given in the text.

Though our resolution represented an improvement, we did not achieve the energy resolution expected on the basis of statistical fluctuations, about 0.5 MeV. Because of the relatively poor energy resolution, only selected targets were used in these experiments. The basis of this selection was that the first excited state of the target nucleus be at sufficiently high energy to enable us clearly to resolve the elastically scattered protons. The targets which were selected were  $\text{Be}^9$ ,  $\text{Ca}^{40}$ ,  $\text{Ni}^{58}$ ,  $\text{Sn}^{120}$ , and  $\text{Pb}^{208}$ . The details of the targets are listed in Table I. The targets were mounted in a small scattering chamber (approximately 13 in. in diameter) to reduce air scattering. This chamber had a Mylar entrance window, and a Mylar exit window which extended over slightly more than half the chamber, allowing one to scatter to approximately

TABLE I. Pertinent data on the targets used in these experiments.

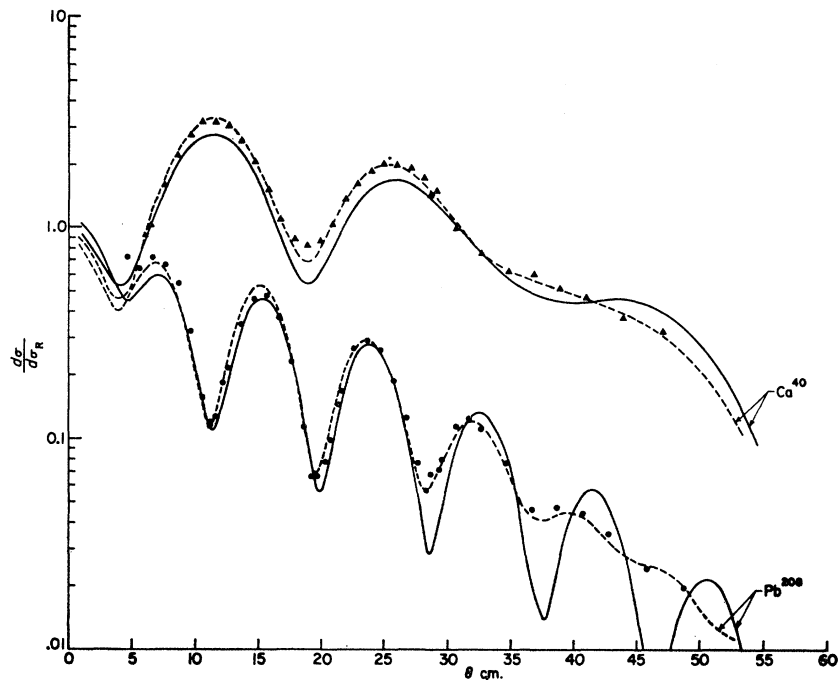
Target	Thickness (mg/cm <sup>2</sup> )	Isotopic purity
$\text{Be}^9$	45.62	98%
$\text{Ca}^{40}$	125.2	95%
$\text{Ni}^{58}$	83.41	99%
$\text{Sn}^{120}$	185.3	99%
$\text{Pb}^{208}$	223.1	91%

$\pm 100^\circ$ . The counter telescope itself was mounted on a 5-ft arm which could be rotated on a track about the center of the scattering chamber to approximately  $85^\circ$  on either side of  $0^\circ$ . The track was ruled in  $\frac{1}{2}^\circ$  increments with a vernier permitting one to set angles to  $0.1^\circ$ . The whole apparatus was mounted on a large table to facilitate alignment with the beam. The position of absolute  $0^\circ$  was determined by measuring the cross section of a high- $Z$  target at small angles on both sides of the beam. Because of the rapidly varying cross section of a high  $Z$  target at small angles, this measurement determined  $0^\circ$  to approximately  $\pm 0.1^\circ$ .

The elastic-scattering cross sections were measured from  $6^\circ$  out to  $\sim 50^\circ$ . All of the cross sections were obtained in relative units with a statistical error which varied from 1% at the small angles to  $\sim 4\%$  at  $50^\circ$ . In addition the cross section for scattering to the 4.43-MeV state in  $\text{C}^{12}$  was measured at  $15^\circ$ ,  $25^\circ$ ,  $35^\circ$ , and  $45^\circ$  with 1% statistical error. This cross section had previously been measured to  $\pm 5\%$  at Orsay,<sup>8</sup> and was used to determine the absolute cross sections. In general the normalization to known cross sections has a distinct advantage when one uses a NaI counter. The

<sup>8</sup> G. L. Salmon *et al.*, Proc. Phys. Soc. (London) **74**, 14 (1962); D. J. Rowe *et al.*, Nucl. Phys. **54**, 193 (1964); J. Garron *et al.*, J. Phys. Radium **21**, 317 (1960).

FIG. 2. See caption for Fig. 1, except that the targets are  $\text{Ca}^{40}$  and  $\text{Pb}^{208}$ .



elastic peak which one obtains in a multichannel analyzer has associated with it a tail arising from reactions which take place in the crystal, producing a substandard pulse. The tail-to-peak ratio appears to follow an  $E^2$  dependence rather well and has a value tail/peak of  $\sim 25\%$  at 160 MeV.<sup>9</sup> If one normalizes his data to known cross sections, it is unnecessary to know the tail-to-peak ratio accurately, since to first order the tail is the same for the standard proton group and the group under question. We need worry only about the difference in the tail/peak ratio resulting from differences in proton energy, because of recoil of the nucleus, which leads to a very small error. As an additional check a measurement of the absolute cross section was made by calibrating the ion chamber with a Faraday cup. The reaction tail was measured by placing the counter in the greatly reduced incident beam. This measurement agreed with the  $\text{C}^{12}$  normalization of 7%. The over-all error was calculated to be  $\pm 5\%$  for the relative cross sections, and  $\pm 7\%$  for the absolute cross sections. Further experimental details can be found in Ref. 7.

### III. RESULTS AND OPTICAL-MODEL ANALYSIS

The angular distributions obtained in this experiment are shown in Figs. 1 and 2, along with the optical-model calculations.<sup>10</sup> Several trends can be seen from looking at the data. First, there is an increase in the oscillatory structure and a movement of the first maximum of the

oscillatory structure to smaller angles with increasing atomic weight  $A$ . Another observation is the lack of the oscillations at large angles. Thus, even for large  $A$  the cross section for angles larger than  $\sim 30^\circ$  is monotonic. It is this feature that leads to difficulties in the optical-model calculation.

In Figs. 1 and 2, two optical-model fits to the data are shown. The solid lines are our fits obtained using the ABACUS program.<sup>11,12</sup> The dashed lines are the fits obtained by Satchler<sup>13</sup> using the HUNTER program. Both programs calculate the nonrelativistic scattering cross section for a given potential. The potential used for these calculations was of the form

$$V = V_{\text{Coul}} + V f_1(r) + iW_D [df_2(r)/dr] + iW f_2(r) + (h/M\pi c)^2 (u_c + iW_s) (1/r) [df_1(r)/dr] \mathbf{l} \cdot \boldsymbol{\sigma},$$

where

$$f_i(r) = [1 + \exp((r - R_i)/a_i)]^{-1},$$

$$R_i = r_i A^{1/3},$$

and  $V_{\text{Coul}}$  is the Coulomb potential resulting from a uniformly charged sphere of radius  $R_c$ . Both programs also have search routines which vary the optical model parameters to minimize  $\chi^2$ , where

$$\chi^2 = \frac{1}{N} \sum_{I=1}^N \left( \frac{\sigma_i^{\text{calc}} - \sigma_i^{\text{expt}}}{\Delta \sigma_i} \right)^2,$$

<sup>11</sup> Program by E. Auerbach, Brookhaven National Laboratory.

<sup>12</sup> The calculations were done both at the MIT Computer Science Center and the University of Maryland Computer Science Center. The calculations at the University of Maryland were supported under NASA Grant N.S.G. 398.

<sup>13</sup> G. R. Satchler (private communication). His  $\chi^2$  have been calculated in a manner slightly different from ours.

<sup>9</sup> D. Measday (unpublished).

<sup>10</sup> Tables of the experimental values are available from the authors.

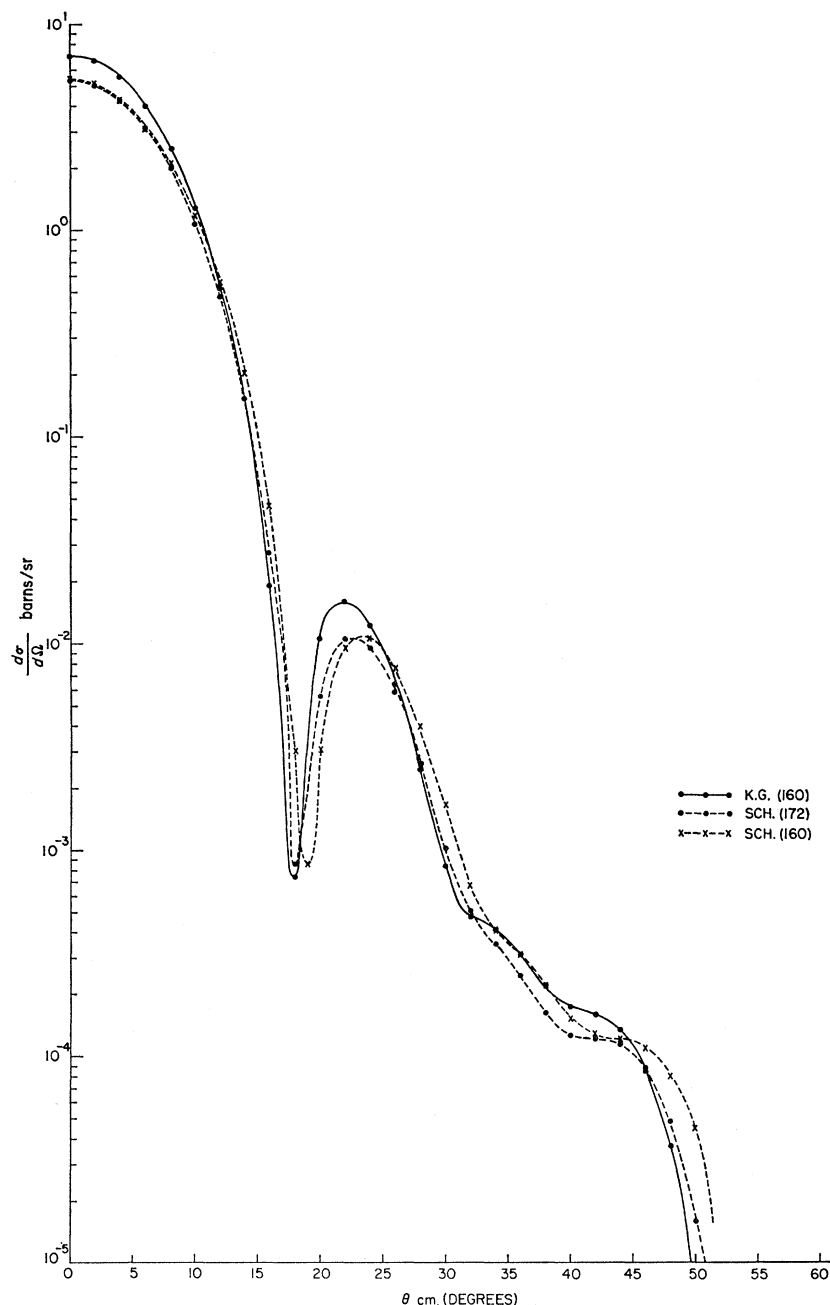


FIG. 3. A comparison of the Klein-Gordon optical-model calculations with a totally nonrelativistic Schrödinger-equation calculation and a Schrödinger-equation calculation with the relativistic center-of-mass momentum. In all three cases the scattering is of neutrons and the optical potentials are the same.

and  $N$  = number of experimental values,  $\sigma_i^{\text{calc}}$  = cross section at angle  $i$  calculated by the program,  $\sigma_i^{\text{expt}}$  = experimental cross section at angle  $i$ , and  $\Delta\sigma_i$  = experimental error in cross section at angle  $i$ .

The optical-model parameters used in the calculations are shown in Table II, along with  $\chi^2$  and the calculated and experimental values for the reaction cross sections. The experimental reaction cross sections are those obtained by Johansson *et al.*<sup>14</sup> at 180 MeV. In Ref. 14

<sup>14</sup> A. Johansson, U. Svanberg, and O. Sundberg, *Arkiv Fysik* **19**, 572 (1961).

the reaction cross sections are shown to be very flat from  $\sim 100$  MeV to  $\sim 1$  BeV, so that one can use the 180-MeV reaction cross sections for 160-MeV proton scattering.

One sees from Figs. 1 and 2 that, in general, Satchler obtains better fits to the data. There is one difference in the two calculations, which arises from the desire to do the kinematics relativistically, even though the Schrödinger equation is nonrelativistic. The  $v/c$  for 160-MeV protons is  $\sim 0.5$ . In our calculations we used an incident energy of 160 MeV. Satchler, however, has

TABLE II. Optical-model parameters. The symbols are defined in the text. All lengths are in fermis ( $10^{-13}$  cm) and energies are in MeV. Rows (a) refer to Satchler's analysis of the data, and rows (b) to the authors' analysis. The reaction cross sections cited are from Ref. 14.

Target		$-V$	$r_1$	$a_1$	$r_e$	$-W$	$r_2$	$a_2$	$-U_s$	$W_s$	$\sigma_{\text{Realc}}$	$\sigma_{\text{expt}}$	$\chi^2$
Be <sup>9</sup>	(a)	-5.40	1.018	0.489	1.89	14.17	1.633	0.385	2.307	4.82	257	186±5	45.5
	(b)	16.2	1.0	0.385	1.3	14.0	1.55	0.40	2.5	1.0	252		17
Ca <sup>40</sup>	(a)	17.5	1.172	0.585	1.32	8.2	1.535	0.483	4.04	0.04	584	524±14	1.8
	(b)	14.54	1.17	0.51	1.3	10	1.50	0.50	2.45	1.0	630		10
Ni <sup>58</sup>	(a)	11.29	1.127	0.648	1.25	9.86	1.49	0.316	3.405	4.067	662	662±19	10.5
	(b)	14.2	1.20	0.52	1.3	10.0	1.45	0.50	2.45	1.0	766		10
Sn <sup>120</sup>	(a)	37.64	1.00	0.71	1.20	16.09	1.342	0.512	4.528	2.205	1339	1165±34	5.1
	(b)	16.2	1.18	0.55	1.3	10.0	1.40	0.50	2.5	1.0	1215		52
Pb <sup>208</sup>	(a)	28.70	1.118	0.702	1.20	17.60	1.308	0.530	0.355	2.98	1866	1790±50	8.3
	(b)	17.0	1.25	0.69	1.3	9.0	1.37	0.70	2.5	1.0	1771		47

used an incident energy such that he gets the correct relativistic center-of-mass wave number. In this way he hopes to include some of the relativistic effects, though he is still using a nonrelativistic Schrödinger equation. In order to estimate the effect of using a nonrelativistic wave number we have done three calculations for Ca<sup>40</sup>. Using the same optical-model parameter but with no spin orbit force, or Coulomb interaction, we have calculated the differential cross section using: (1) the Schrödinger equation with 160-MeV incident energy; (2) the Schrödinger equation with an incident energy of 172.25 MeV, which gives the correct relativistic center-of-mass momentum; (3) the Klein-Gordon equation with the potential entered as the fourth component of a four-vector.<sup>11</sup> The results of the calculations are shown in Fig. 3. Assuming that such a Klein-Gordon equation is a correct relativistic generalization of the Schrödinger equation, one sees that only using the correct momentum in a Schrödinger equation calculation does not reproduce the Klein-Gordon result. Both Schrödinger equation calculations differ from the Klein-Gordon calculation, and are similar to each other, giving no evidence that one calculation is better than the other. It should be mentioned that the use of the correct relativistic momentum does give better agreement with respect to the position of the peak, but this can easily be corrected in the 160-MeV calculation by a slight change in radius.

In any case, since the differences between the Klein-Gordon and Schrödinger equation results are not large, we believe that, even at energies this high, optical-model parameters are still meaningful, phenomenologically. A study of Table II shows that the imaginary-well radius is sizeably larger than the real-well radius. This was necessary in order to reduce the oscillatory structure in the large angle region, and has been found in

high-energy proton-nucleus scattering analysis by others.<sup>3,13,15</sup> Table III shows that the difference in radii between the real and imaginary parts of the potential, defined by,

$$\Delta R = (r_2 - r_1)A^{1/3}$$

is approximately constant for the nuclei studied. These nuclei span the periodic table and it would therefore appear that the difference in radii represents a general nuclear-structure phenomenon. In this comparison we have neglected any weighting arising from the fact that the depth of the imaginary well varies, as does  $a_i$ , from nucleus to nucleus.

In terms of the impulse approximation, one might expect the real radius to be equal to the imaginary radius. That is, because of the high energy, and therefore small  $\lambda$ , one expects the scattering potential to be the sum of the two-body scattering potentials. Therefore, the nucleon-nucleus scattering potential, both real and imaginary parts, should reflect the distribution of nucleons in the nucleus. Starting with this assumption, we first attempted to keep the real and imaginary wells of the same shape. However, after extensive scans over

TABLE III. The difference in half-value radii between the real and imaginary parts of the optical potential.  $\Delta R_a$  refers to Satchler's analyses and  $\Delta R_b$  refers to the author's analysis. All units are  $10^{-13}$  cm.

	$\Delta R_a$	$\Delta R_b$
Be <sup>9</sup>	1.28	1.15
Ca <sup>40</sup>	1.24	1.13
Ni <sup>58</sup>	1.42	0.97
Sn <sup>120</sup>	1.68	1.08
Pb <sup>208</sup>	1.13	0.71
	$\langle \Delta R \rangle = 1.35$	$\langle \Delta R \rangle = 1.01$

<sup>15</sup> P. E. Hodgson, Phys. Rev. Letters **6**, 358 (1961).

the other parameters, we concluded the one cannot reduce the oscillatory structure in the large-angle region, when using imaginary and real wells of the same shape. Taking the imaginary-well radius larger than the real-well radius ( $r_2 > r_1$ ), we could reduce the oscillatory structure at larger angles and thereby improve the fits. Increasing the imaginary-well radius, however, leads to another difficulty—that of a predicted reaction cross section which is too large, especially for the lighter elements. Attempts to reduce  $\sigma_{\text{reaction}}$  maintaining a good fit to the angular distributions met with failure. Good fits to the data always resulted in a reaction cross section which was too large. Thus, we finally fitted the differential cross section keeping the  $\sigma_{R \text{ calc}}$  as small as possible but not fitting  $\sigma_{R \text{ expt}}$ . This same difficulty was met by Satchler and Haybron<sup>3</sup> whose  $\sigma_{R \text{ calc}}$  were also too large, and generally agreed with those obtained in this analysis.

One might suspect that there could be difficulties, because of the use of the Schrödinger equation. Again we attempt to investigate this using the Klein-Gordon equation. The Klein-Gordon calculations of the differential cross section are very similar in shape to the Schrödinger calculations; they give too much oscillation for equal radii, and smooth larger angle cross sections for an imaginary radius larger than the real radius. Thus, it seems very unlikely that a correct relativistic treatment will change the result that it is necessary to use a larger imaginary radius. In this connection it has been pointed out by Elton<sup>16</sup> that if one introduces into the Dirac equation the optical potential as the fourth component of a four-vector, and if the energy of the particle is large compared to the potential depth, the relativistic corrections can be absorbed into the strengths of the central and spin-orbit potentials. The resultant equation is a slightly modified Schrödinger equation with, however, relativistic kinematics.

In Ref. 1 it is shown that the momentum dependence of the nucleon-nucleon cross sections permits a difference in the real and imaginary optical-potential-well sizes. In that paper an approximation is made to include the dependence of the nucleon-nucleon scattering coefficients on the momentum transfer. The rms scattering radius is written as

$$R^2 = R_e^2 + R_N^2,$$

where  $R_e$  is the radius measured in electron-nucleus scattering experiments, and  $R_N$  is a term which depends on the second derivative of the nucleon-nucleon scattering coefficients with respect to momentum transfer. In calculations of Ref. 1 they find that  $R_N^2$  for the imaginary radius is approximately 0.1 F<sup>2</sup> larger than  $R_N^2$  for the real radius at 147 MeV. This value should be compared to our  $\langle \Delta R \rangle^2$  of 1 or 1.8 F<sup>2</sup> using Satchler's

parameters. However, they used Gammel-Thaler phase shifts to derive their nucleon-nucleon scattering coefficients. We have evaluated the second derivative of the scattering amplitude using the Yale phase shift sets YLAM and YLAN3M.<sup>17</sup> This calculation gave approximately the same results as the calculation of Ref. 1.

One must also consider that the various approximations used in driving an optical potential from the impulse approximation may not be satisfied in that the momentum of the incident nucleon is not large compared to that of the target nucleons.<sup>18</sup> That the impulse approximation in the sense of Ref. 1 is valid even at the relatively low energies considered here is born out by the fact that the total cross section is known to be made up very largely from what appears to be quasielastic scattering as described by Wolff.<sup>19</sup> This process will be discussed in a subsequent paper, and some discussion may be found in Ref. 7. It has recently been suggested by Rowe<sup>8</sup> and Clegg<sup>20</sup> that the "off-the-energy-shell" terms, which can be present in nucleon-nucleus scattering as distinguished from free nucleon-nucleon scattering, may be present for large momentum transfers. This point has not been investigated, but inasmuch as these terms arise from the coupling of the struck nucleon to the rest of the nucleus they may very well lead to special properties of absorptive channels, or the imaginary well.

A different approach to the calculation of high-energy proton scattering, avoiding the question of an optical model and its parameters, has been made by Frahn and Venter.<sup>21</sup> In their calculations a functional form, appropriately parametrized, for  $\eta$ , the coefficient of the outgoing wave in the partial-wave expansion, was used. Treating  $l$  as a continuous variable they integrate over it rather than sum and derive a closed-form expression for the differential cross section, polarization, and the reaction cross section. For high-energy proton scattering they have made use of their " $\nu$  model" to limit the parameter space, the " $\nu$  model" being suggested by the polarization data, and having only five parameters. The five parameters are then adjusted to fit the data of Ref. 2. Their calculations do reproduce the smoothness in cross section at large angles and give reasonable fits to all the data. However, their fits to the data are not as good as those obtained by Satchler and Haybron<sup>3</sup> by their optical-model analysis. Furthermore, the  $\eta_l$  from the optical-model analysis are not the same as those of Frahn and Venter. In particular, one does not get the pronounced peaking in the  $\text{Im}\eta_l$  from the

<sup>17</sup> G. Breit *et al.*, Phys. Rev. **128**, 826 (1962); M. H. Hull *et al.*, *ibid.* **128**, 830 (1962).

<sup>18</sup> This criterion on the impulse approximation is valid insofar as it expresses the more correct criterion that the time of collision be short compared to the characteristic time of the motion of the struck particle.

<sup>19</sup> P. Wolff, Phys. Rev. **87**, 434 (1952).

<sup>20</sup> A. B. Clegg, Nucl. Phys. **66**, 185 (1965).

<sup>21</sup> R. H. Venter and W. E. Frahn, Ann. Phys. (N. Y.) **27**, 385 (1964).

<sup>16</sup> L. R. B. Elton (private communication). See also M. L. Goldberger and K. M. Watson, *Collision Theory* (John Wiley & Sons, Inc., New York, 1964).

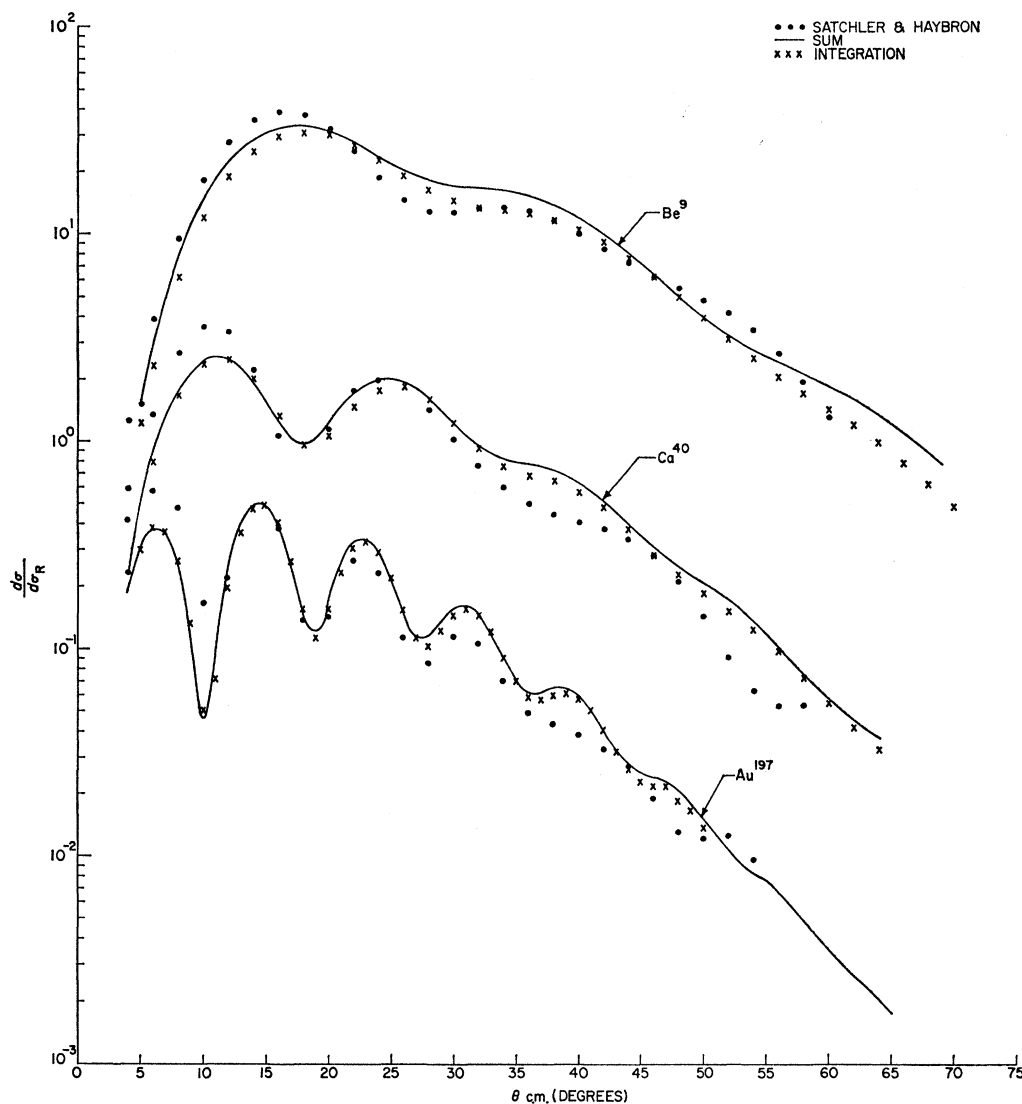


FIG. 4. A comparison of the Frahn-Venter calculation with their modified parameters using a summation (—); the integration (×) those authors use; and optical-model calculations (●) at 182 MeV. The reaction cross section calculated by the summation differs by less than 1% from that calculated by the integration.

optical-model analysis that one would get from the derivative of a Saxon shape, which they use for the imaginary part of  $\eta$ . One might also worry about Frahn and Venter's integration over  $l$ ; i.e., as to its effect in smoothing the differential cross section. We therefore compared the results for integration over  $l$  to summing over  $l$ . These calculations are illustrated in Fig. 4. As one might expect, the largest differences were seen in  $\text{Be}^9$ , where there are only about 18 partial waves which enter the calculation. The angular distributions from the two calculations are very similar, and the only essential difference is in magnitude. The important point is that the optical-model calculations of Satchler and Haybron give better fits to the data, though further adjustment of the parameters in Frahn

and Venter's calculation would almost certainly improve their fits.

One can see from Fig. 4 that the Frahn and Venter calculations are too small in magnitude, particularly in the region of the first maximum. This effect is more pronounced for the heavier nuclei, and is probably due to the fact that these calculations do not include Coulomb effects.

In the case of In and Au, Frahn and Venter give a set of modified values for their parameters (also within the framework of the " $\nu$ -model") which represent a significantly better fit to the data than their "standard" set. These modified parameters, however, also predict reaction cross sections which are considerably higher than the experimental values. The modified parameters

have been used in the curves shown in Fig. 4. As the authors point out, the reaction cross section is most sensitive to their parameter  $\bar{\epsilon}_1$ , which was not changed from the "standard" value. To obtain the necessary reduction in cross section to keep agreement with experiment on the reaction cross section it is necessary in the case of Au to make  $\bar{\epsilon}_1=0.25$ , instead of 0.015. This lowers peak cross sections in the differential cross section by about 35% but does not shift the locations of the maxima or minima. The polarization is increased also but by a smaller quantity, however it is already 30–50% greater than experiment. It may still be possible to obtain a better fit to the data at 182 MeV by varying the other parameters, but this was not done in the present work.

#### IV. CONCLUSIONS

We have measured the elastic-scattering differential cross sections from a variety of nuclei spanning the periodic table. We have shown the appropriateness of an optical-model description, and in Table II summarized such analyses. We have also indicated that one can in all probability determine a set of phase-shift parameters following Frahn and Venter. This parametric representation does not give quite the same phase-shift-versus-angular-momentum function as the optical-model analyses. As in the case of low-energy neutron scattering,<sup>22</sup> we have found that the optical-

model analysis yields an imaginary potential of greater radial extent, by about  $1f$ , than that of the real potential. Reference 22 lists a number of the theoretical papers dealing with the effect of the Pauli principle at low energies. These papers show that as the energy is increased the absorptive fringe should decrease. At present there is no quantitative explanation of the present observation on the existence of such a fringe at high energies.

*Note added in proof.* Recent calculations have been carried out by one of the authors (P. G. R.) using the HUNTER program which permits the spin-orbit well to be decoupled from the central well. These calculations indicate that it is possible to obtain a good fit to the  $\text{Ca}^{40}$  data with equal real and imaginary radii, but with a spin-orbit radius much smaller than the values given in Table II.

#### ACKNOWLEDGMENTS

The authors would like to thank A. Koehler for his help with operating and maintaining the Harvard Cyclotron, Dr. B. Gottschalk for the use of much of his equipment and for his helpful suggestions, and Dr. R. Satchler for his comments on this work and for permission to quote his results. Dr. R. Bassel's assistance in a calculation is also acknowledged. A particular debt of gratitude is owed E. Auerbach for his ABACUS program and its modifications.

<sup>22</sup> C. D. Zafiratos *et al.*, Phys. Rev. Letters **14**, 913 (1965).